J Mater Sci (2009) 44:5120–5126
DOI 10.1007/s10853-009-3455-2

FERROELECTRICS

Low-frequency magnetoelectric interactions in single crystal and polycrystalline bilayers of lanthanum strontium manganite and lead zirconate titanate

N. Zhang · G. Srinivasan · A. M. Balbashov

Received: 8 March 2009 / Accepted: 31 March 2009 / Published online: 17 April 2009

Abstract The magnetoelectric (ME) characterization of bilayers of lead zirconate titanate (PZT) and single crystal or hot-pressed polycrystalline lanthanum strontium manganite (LSMO) are discussed. Data on ME voltage coefficient have been obtained as a function of strength and orientation of bias magnetic field H, temperature, and frequency. The bilayers exhibit superior ME coupling compared to thick film multilayer composites and the strongest ME interactions are measured for samples with single crystal LSMO. Bilayers with single crystal LSMO show strong dependence of ME coefficient on H orientation and temperature, with a maximum value of 190 mV/cm Oe at 86 K. The frequency dependence of ME coefficient reveals a resonance enhancement due to radial acoustic modes. There is excellent agreement between theory and data for the H variation of ME coefficients.

Introduction

Magnetoelectric (ME) multiferroics have attracted considerable attention in recent years for studies on the physics of ME interactions and for useful technologies [1]. Although the strength of ME interactions in single-phase multiferroics is generally weak at room temperature, composites of ferromagnetic and piezoelectric phases show very strong interactions [2]. In such systems, the electromagnetic coupling occurs via mechanical stress. A layered configuration for ME composites has several advantages, such as reduction in leakage currents, over bulk sintered composites. An ideal ferromagnet for a layered composite must have negligible resistance so that there is no loss of piezoelectric voltage. Several such systems, including ferrite, terfenol-D, or transition metals or alloys for the magnetic phase, and lead zirconate titanate (PZT) or lead magnesium niobate–lead titanate (PMN-PT) for the piezoelectric phase, have been investigated in recent years [1–10].

Investigations on the nature of magnetoelectric interaction in a bilayer of ferromagnetic lanthanum strontium manganite and piezoelectric lead zirconate titanate are discussed. Ferromagnetic manganites have metallic conductivity and structural and thermal property compatibility with PZT, key ingredients for obtaining defect free composites with good interface coupling [11]. There have been very few studies on magnanite-piezoelectric systems [12–15]. Our earlier study on manganite-PZT resulted in the first report on magnetoelectric (ME) coupling in the system [12]. Bilayers and multilayers of $La_{0.7}Sr_{0.3}MnO_3$ (LSMO)-PZT and $La_{0.7}Ca_{0.3}MnO_3$ (LCMO)-PZT were synthesized. The strength of the ME coupling was measured as a function of bias magnetic field, frequency, and temperature. The coupling was found to be stronger in LSMO-PZT than in LCMO-PZT, and was weaker in multilayers compared to bilayers. The measured ME voltage coefficient α_E, however, was *an order of magnitude smaller* than theoretical values. Although XRD shows no impurity phases, the ME parameters were found to be very sensitive to sintering temperature, an observation that pointed to the interface diffusion as the possible cause of poor ME effects [12].

N. Zhang · G. Srinivasan (✉)
Physics Department, Oakland University, Rochester, MI 48309, USA
e-mail: srinivas@oakland.edu

A. M. Balbashov
Moscow Power Engineering Institute, Moscow 111250, Russia

Here we report on significantly enhanced ME interactions in LSMO-PZT bilayers of single crystal or polycrystalline LSMO and polycrystalline PZT. For polycrystalline samples, sol–gel derived powders of LSMO were processed by hot-pressing at 1300 K, followed by final sintering at 1500–1650 K to obtain dense samples with best magnetic parameters. Single crystals of LSMO were grown by floating zone techniques. Bilayers were made by bonding disks of the two phases. We measured in the bilayers a substantial enhancement in the strength of low-frequency ME coupling, by a factor of 3–8 compared to sintered multilayers. The strongest ME coupling occurs in samples with single crystal LSMO and the coupling is found to be dependent sensitively on the orientation of bias magnetic field H. A resonance enhancement in ME coupling occurs when the frequency of the ac magnetic field is tuned to acoustic modes in the samples. Details on these results are provided in the following sections.

Synthesis of manganite and structural and magnetic characterization

The manganite perovskites $La_{1-x}M_xMnO_3$ where M is a divalent alkaline-earth (e.g. Ca, Ba, Sr) have shown several important phenomena including colossal magnetoresistance, charge ordering, magnetic field induced structural transitions, and giant magnetostriction [11]. The parent oxide without M-ions is an antiferromagnetic insulator. For specific compositions, the divalent substitution leads to ferromagnetic order and metallic conductivity due to the double exchange between Mn^{3+} and Mn^{4+} ions. Strontium substituted manganite is ferromagnetic for $x > 0.1$. The Curie temperature T_c varies from a minimum of 150 K for $x = 0.1$ to a maximum of 375 K for $x = 0.35$–0.45 [11].

Polycrystalline samples of $La_{0.7}Sr_{0.3}MnO_3$ (LSMO) were prepared from nanoparticles obtained by sol–gel techniques as described below [13]. Stoichiometric amounts of La_2O_3, $Sr(NO_3)_2$, and Mn_2O_3 were added to citric acid and dissolved in dilute nitric acid. The solution was then heated at 400–500 K for 2 h to obtain a homogeneous liquid free of any suspensions. Further heating for several hours at 370 K was carried out until the solution was transformed into a dry gel. The gel was ground into fine powder and heated at 500–700 K for 12 h. The powder was pressed into pellets of 10 mm in diameter and 5–6 mm in thickness and hot-pressed at 7 MPa and 1300 K for 1 h. An applied test systems hot-press and dies made of alumina were used. Further sintering of the hot-pressed samples at 1500–1650 K was necessary for dense, stoichiometric LSMO samples with best magnetic parameters.

Single-crystal (001) LSMO were grown by the floating zone melting method. Single-crystal seeds having a length of 10 mm and in-plane size of 2×1 mm^2 were used. The crystals were grown under oxygen pressure of approximately 55 atm and the crystal rotation velocity of 40 rpm. The crystallization speed was 10 mm/h. The crystals were then annealed in oxygen flow at the temperature of 1300 °C.

Detailed structural studies were carried out on our samples. X-ray diffraction data on polycrystalline LSMO showed the absence of any impurities. Single crystal LSMO rods had the [001] [or the c-axis] orientation along the axis and were cut to 0.5 mm thick slabs for use in bilayers.

Techniques for magnetic characterization included magnetization, ferromagnetic resonance (FMR) at 9.4 GHz, and magnetostriction. We refrain from a detailed discussion on the magnetic properties, but provide here important data relevant to this study on ME interactions. For polycrystalline LSMO Fig. 1 shows room temperature saturation magnetization M_s measured with a Faraday balance and FMR line-width ΔH estimated from derivative of the absorption using a Varian ESR spectrometer and a TE_{102} reflection type cavity. The data are for LSMO sintered at 1300–1650 K. Samples sintered at or above 1580 K show expected M_s values. The lowest ΔH is measured for samples sintered at the same temperature range. Since ΔH is a sensitive indicator of phase homogeneity, porosity, and any defects, one can conclude from the data in Fig. 1 that sintering at or above 1580 K results in samples with best magnetic parameters for use in layered ME composites. Similar FMR measurements on single crystal LSMO showed evidence for in-plane anisotropy in the (001) plane.

The magnetic parameter of importance for ME coupling is the magnetostriction λ. The dynamic ME coupling is directly proportional to the piezomagnetic coefficient defined by $q = \delta\lambda/\delta H$. Figure 2 shows representative data

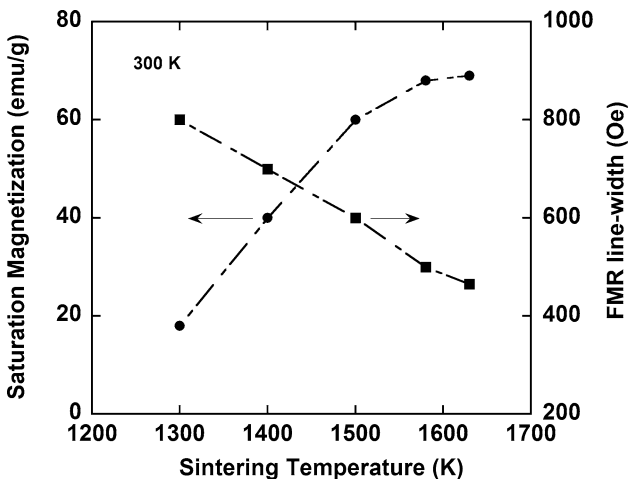

Fig. 1 Room temperature saturation magnetization and ferromagnetic resonance line-width at 9.4 GHz for $La_{0.7}Sr_{0.3}MnO_3$ (LSMO)

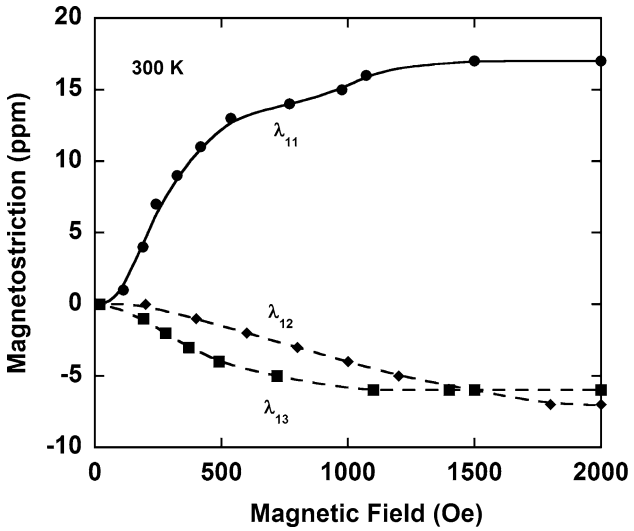

Fig. 2 Magnetostriction λ versus H data at room temperature for LSMO sintered at 1580 K. With the disk sample in (1,2) plane, measurements of λ were made for (i) H along axis of the strain gage: λ_{11}, H in-plane and perpendicular to strain gage: λ_{12} and (iii) H- perpendicular to the sample plane :λ_{13}. The lines are guides to the eye

on the bias magnetic field H dependence of magnetostriction λ in polycrystalline LSMO sintered at 1580 K. The data were obtained by the standard strain gage technique. The measurements were made for H parallel or perpendicular to the plane of a disk shaped sample in (1,2) plane. The magnetostriction was measured along direction-1 for H directed along the primary axes (λ_{11}, λ_{12}, or λ_{13}). The parallel magnetostriction λ_{11} is positive. For most materials λ_{11} is expected to be a factor of two larger than λ_{12} or λ_{13}, as is the case for LSMO [12]. Saturation of λ occurs for fields above 1.5 kOe.

Magnetoelectric characterization

Bilayers of polycrystalline LSMO and PZT were made by bonding 9 mm diameter and 0.5 mm thick disks of manganite and commercial PZT [16]. Single crystal LSMO of dimensions $4 \times 4 \times 0.5$ mm^3 was bonded to PZT of the same dimensions were also used for ME studies. PZT was first poled by heating to 425 K and cooling back to room temperature in an electric field of 30–50 kV/cm perpendicular to the sample plane. It was then bonded to LSMO. For bonding we used the following procedures: (i) a quick-dry epoxy, (ii) silver epoxy with hardener, and (iii) slow-dry epoxy resin with hardener. The best results reported here were obtained for quick dry epoxy bonded samples.

For ME characterization, we measured the electric field produced by an alternating magnetic field applied to the

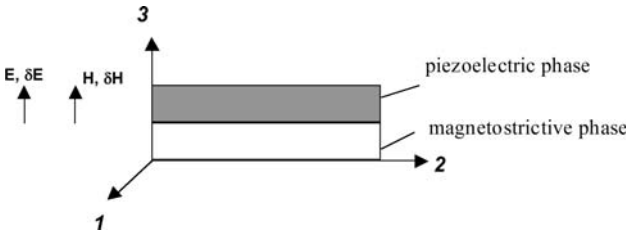

Fig. 3 Schematic showing a piezoelectric-magnetostrictive bilayer in the (1,2)-plane. The poling field E is along the sample thickness (direction-3). For the transverse magnetoelectric voltage coefficient measurements, the bias field H and the ac magnetic field δH are parallel to each other and to the sample plane and the induced electric field δE is measured perpendicular to the sample plane. For the longitudinal case, all the fields are along the direction-3

composite. The samples were positioned in a measurement cell and subjected to a bias magnetic field H and an ac magnetic field δH. The voltage δV across the sample was amplified and measured with an oscilloscope or a lock-in-amplifier. The ME voltage coefficient was estimated from $\alpha_E = \delta E/\delta H = \delta V/t\delta H$ where t is the thickness of PZT. The measurements were done for two different field orientations as shown in Fig. 3. The transverse coefficient $\alpha_{E,31}$ was measured for the magnetic fields H and δH along direction-1 (parallel to the sample plane) and perpendicular to δE (direction-3). The ME coefficients were measured as a function of H, frequency, and temperature. A liquid-helium glass dewar and a nonmetallic sample insert were used for studies on temperature dependence of ME effects.

Polycrystalline LSMO-PZT

We carried out a systematic investigation on the dependence of the strength of ME interactions on (i) the bias magnetic field, (ii) temperature, and (iii) frequency of ac magnetic field. Figure 4 shows the H dependence of the transverse coefficient $\alpha_{E,31}$ and the longitudinal coefficient $\alpha_{E,33}$. The data are for 300 K and a frequency of 100 Hz for the ac magnetic field. Consider the transverse coupling first. As H is increased $\alpha_{E,31}$ increases in magnitude and peaks at 150 Oe. With further increase in H, $\alpha_{E,31}$ shows a rapid decline and then a gradual decrease to zero. The longitudinal coefficient $\alpha_{E,33}$ shows a similar rise-and-fall as H is increased with a peak at 1800 Oe. But the magnitude of the longitudinal coupling is quite small compared to $\alpha_{E,31}$.

The α_E values in Fig. 4 are of the same order of magnitude as in similar layered composites. For comparison, $\alpha_{E,31}$ is 400 mV/cm Oe for nickel ferrite-PZT, 4680 mV/cm Oe for Terfenol-PZT, and 50–600 mV/cm Oe for samples with Ni, Co, or Ni and PZT [1, 17]. Now we compare the results in Fig. 4 with the strength of ME interactions in thick film multilayers of manganite-PZT [12]. We synthesized bilayers and multilayers of $La_{0.7}Sr_{0.3}MnO_3$-PZT by sintering

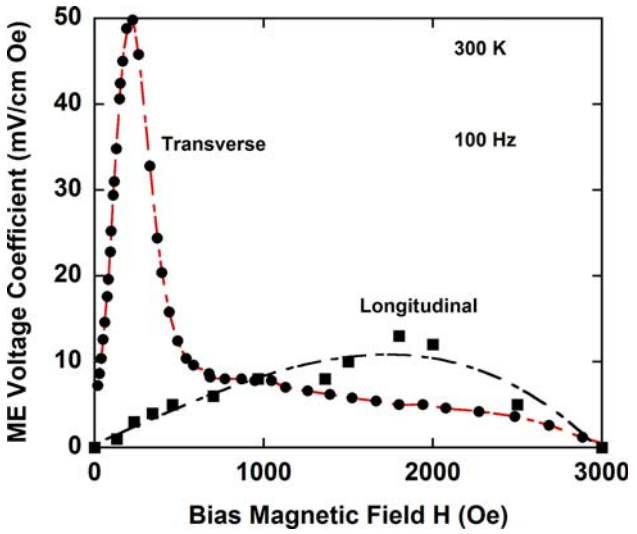

Fig. 4 Static field dependence of room temperature transverse and longitudinal ME voltage coefficients for polycrystalline LSMO-PZT bilayer. The lines are guides to the eye

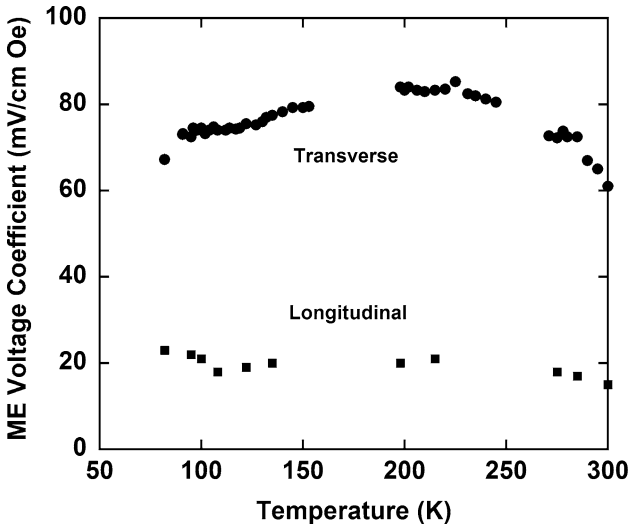

Fig. 5 Temperature dependence of the peak transverse and longitudinal coefficients, $\alpha_{E,31}$ and $\alpha_{E,33}$ respectively, for the polycrystalline LSMO-PZT bilayer. Values of α_E are for the bias field H corresponding to maximum value in the ME effect. The temperature dependence is for a frequency of 100 Hz

20–40 μm thick films and studied ME effects at low frequencies showed α_E that were a factor of two smaller than the data in Fig. 4. Further weakening of ME coupling occurred in multilayers processed at high temperatures and was accompanied by deterioration of magnetic and electrical parameters for the samples. These observations were evidence for diffusion of metal ions from manganite and PZT across the interface. It is quite clear from the data in Fig. 4 that a bonded LSMO-PZT is free of such problems, leading to a strong ME coupling.

The temperature dependence of the strength of ME interactions is considered next. The variation with temperature of the ME coefficients at 100 Hz are shown in Fig. 5. The data correspond to peak values in α_E vs. H as in Fig. 4 at each temperature. The longitudinal effect remains temperature independent, but the transverse coefficient shows an initial increase with temperature as the sample is warmed up from 80 K. The maximum in the coupling strength occurs at 225 K. Further increase in temperature results in a decrease in $\alpha_{E,31}$. We attribute these changes to temperature dependence of material parameters, in particular the magnetostriction.

Finally, the frequency dependence of α_E was studied. The bias field was first set at the field corresponding to maximum in α_E. For examples, these correspond to 150 Oe and 1.8 kOe for the data on transverse and longitudinal coupling in Fig. 4. The voltage coefficients were then measured as the frequency f of the ac field δH was varied. Typical α_E vs. f profiles at room temperature for transverse fields are shown in Fig. 6. Upon increasing f, $\alpha_{E,31}$ increase gradually with minor peaks at 80 kHz and 170 kHz. At

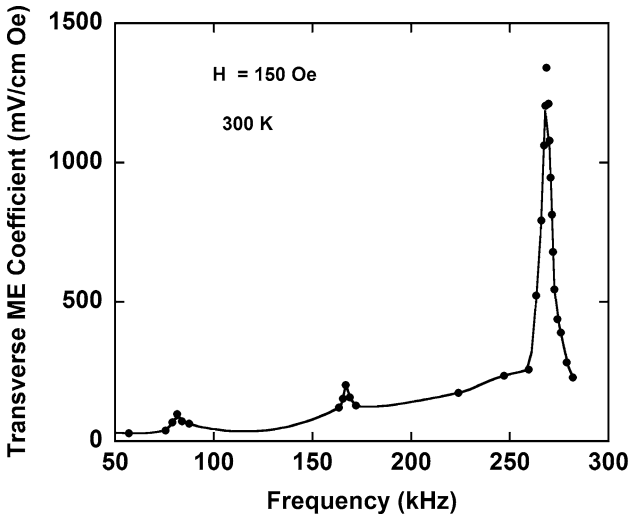

Fig. 6 Frequency dependence of transverse ME voltage coefficients for polycrystalline LSMO-PZT. The bias field H was set for maximum ME coupling (Fig. 3). The lines are guide to the eye. The resonance frequency corresponds to the electromechanical (EMR) for PZT in the composite

higher f, we observe a rapid increase in $\alpha_{E,31}$ to a maximum of 1300 mV/cm Oe at 268 kHz. The profile thus shows resonance with $f_r = 268$ kHz and a width $\Delta f = 3$ kHz, corresponding to a quality factor $Q = 90$. A similar resonance occurred for longitudinal fields. The resonance occurs at the same frequency as for the transverse fields, but with a much smaller maximum α_E (=350 mV/cm) Oe and a lower Q (=50) compared to the transverse fields. The origin of these resonances is discussed in section "Discussion".

Single crystal LSMO-PZT

Measurements on single crystal LSMO-PZT showed a substantial strengthening of ME interactions compared to polycrystalline bilayers. The longitudinal ME coupling was quite weak and not discussed here. The transverse coupling strength was measured as a function of H, the orientation in the bilayer plane, i.e. (001) of LSMO, and temperature. Consider first the data on $\alpha_{E,31}$ vs. H at room temperature and $f = 100$ Hz in Fig. 7. One observes a rapid increase in $\alpha_{E,31}$ with H to a peak value of 135 mV/cm Oe, followed by a sharp drop to zero for $H = 300$ Oe. This maximum value for $\alpha_{E,31}$ is a factor of 2.7 higher than for polycrystalline bilayers and an order of magnitude higher than for thick film multilayers [12]. We also measured a substantial anisotropy in $\alpha_{E,31}$ with the orientation of H in the bilayer plane. Figure 7 shows the peak value of $\alpha_{E,31}$ as a function of the in-plane θ. We define $\theta = 0$ as the field angle corresponding to maximum in $\alpha_{E,31}$. The data show a decrease in the ME coefficient with increasing θ and reaches a minimum at 90°. For $\theta = 90$–180°, the variation in $\alpha_{E,31}$ was a mirror image of the data in Fig. 7 with a 180° symmetry in $\alpha_{E,31}$ vs. θ.

We then obtained data on $\alpha_{E,31}$ vs. H for $\theta = 0$ as the sample was cooled down to 86 K and results on $\alpha_{E,31}$ vs. H are shown in Fig. 8 for a series of temperatures. A general decrease in $\alpha_{E,31}$ with a decrease in temperature is observed with $\alpha_{E,31}$ reaching a value of 58 mV/cm Oe at 86 K. Further investigations were then carried out on the dependence of $\alpha_{E,31}$ on θ at the lowest temperature and the results are shown in Fig. 9. With increasing θ a substantial broadening of $\alpha_{E,31}$ vs. H is obvious in Fig. 9. The peak value of $\alpha_{E,31}$ initially increases with θ and shows a maximum of

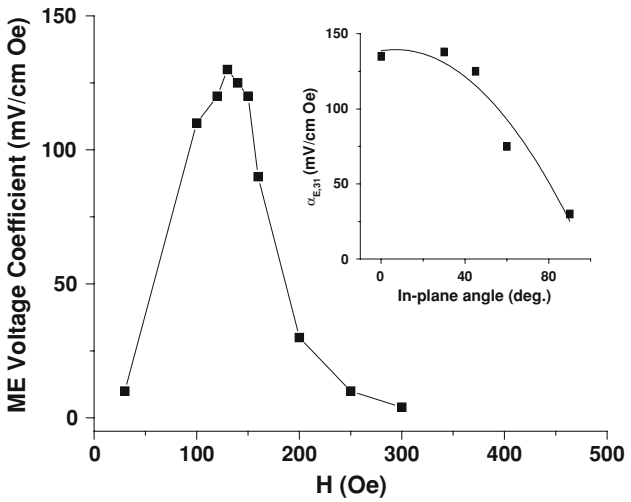

Fig. 7 Transverse ME voltage coefficient measured at 100 Hz and 298 K as a function of H for single crystal LSMO-PZT bilayer. The inset shows the peak value of $\alpha_{E,31}$ as a function of the in-plane angle θ for H

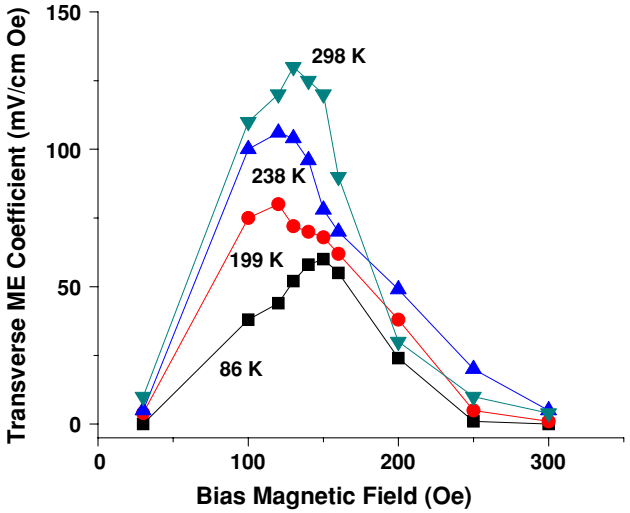

Fig. 8 Data as in Fig. 6 for $\theta = 0$ and as a function of temperature

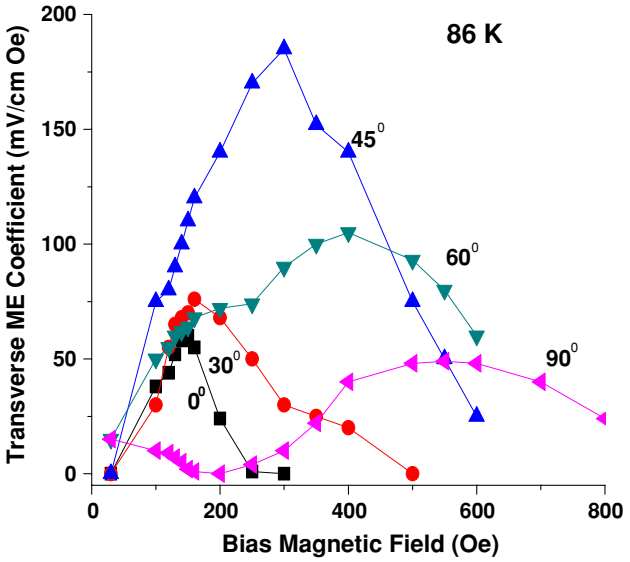

Fig. 9 Transverse ME coefficient versus H at 86 K for a series of in-plane H orientations

190 mV/cm Oe at $\theta = 45°$. Further increase in θ is accompanied by a decrease in the ME coefficient to a minimum value for $\theta = 90$. With increasing θ one also observes an up-shift in the bias field corresponding to maximum ME coefficient. Thus the strongest ME coupling in single crystal bilayer is measured at the lowest temperature of 86 K for $\theta = 45°$.

Discussion

The magnitude and the field dependence in Figs. 4, 5, 6, 7, 8, and 9 are related to magnetostriction and piezomagnetic effects in LSMO. We developed a model for ME effects in

layered samples for an understanding of the ME effects [12]. The composite was considered as a homogeneous medium with piezoelectric and magnetostrictive subsystems. An interface parameter k was introduced to define the interface coupling of mechanical deformation. Expressions for longitudinal and transverse ME coefficients were obtained using the solutions of elastostatic and electrostatic equations [12]. According to the model, $\alpha_{E,33}$ is expected to be quite small due to weak λ_{13} and demagnetizing fields. Such a prediction is in agreement with the data in Fig. 4. We estimated $\alpha_{E,31}$ vs. H for the polycrystalline LSMO-PZT using bulk values for material parameters [12] and $q = \delta\lambda/\delta H = q_{11} + q_{12}$ obtained from λ vs. H data in Fig. 2. Theoretical estimates of transverse ME coefficients are shown in Fig. 10 and compared with the data (of Fig. 4). The estimates are for an interface coupling $k = 0.2$. There is good between theory and data, for both the magnitude of $\alpha_{E,31}$ and its H dependence.

The most important observation in Figs. 4, 5, 6, 7, 8 is the strongest ME coupling measured for samples with single crystal LSMO and could be attributed to several magnetic and material parameters. The most appropriate magnetic parameter for ME coupling is the magneto-mechanical coupling k_m that is given by $k_m = (4\pi\lambda'\mu_r/Y)^{1/2}$ where λ' is the dynamic magnetostrictive constant that is analogous to q, μ_r is the reversible (or ac) permeability, and Y is the Young's modulus. Thus additional measurements of elastic and magnetic parameters are necessary on single crystal LSMO for a full understanding of the origin of strong magneto-mechanical coupling.

The data in Figs. 7 and 9 on $\alpha_{E,31}$ versus in-plane orientation of H could very well be due to variations in magnetostriction and permeability. There are two types of magnetostriction in a ferromagnet: (i) Joule magnetostriction associated with domain movements and (ii) volume magnetostriction associated with magnetic phase change. The volume magnetostriction is not important in the present situation since it is significant only at temperatures close to the Curie temperature and for high fields. In ferromagnets, domains are spontaneously deformed in the magnetization direction. Under the influence of a bias field H and ac field δH, wall motion and rotation contribute to the Joule magnetostriction. Since the ME coupling involves dynamic magnetomechanical coupling, key parameters for strong ME coupling are high permeability due to unimpeded domain wall motion, domain rotation, and a large λ. Magneto-optical imaging and X-ray topography studies on LSMO single crystals reveal a strong correlation between magnetic domain structure and twin domains formed due to rhombohedral deformation of the cubic cell of LSMO [18]. Such twin domains and their influence on magnetic domains, permeability, and magnetostriction are the likely cause of observed variations in the ME coefficient with in-plane orientation of the bias magnetic field.

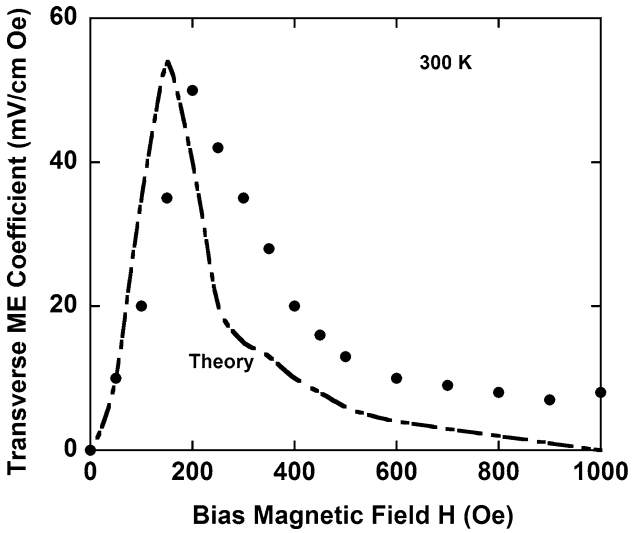

Fig. 10 Comparison of theoretical estimates and data for transverse ME voltage coefficient in polycrystalline LSMO-PZT bilayers. The lines are theoretical values for an interface coupling parameter $k = 0.2$

Finally, we consider the frequency variation of the ME coefficient as in Fig. 6. We identified the resonance enhancement in the ME coupling at f_r with electromechnical resonance (EMR) in PZT. The resonance is characterized by a discontinuity in impedance versus f data [19–21]. It is obvious from Fig. 6 that EMR leads to a very significant enhancement in the strength of ME coupling, by a factor of 25 compared to the low frequency value (Fig. 4). The resonance in ME coefficient occurs when the ac field is tuned to EMR. We developed a model for magnetoelectric interactions at EMR [22]. In a bilayer in the form of thin disk of radius R the ac magnetic field induces harmonic waves in the radial or thickness modes. The model considers radial modes for transverse or longitudinal fields. An averaging procedure was employed to obtain the composite parameters and the ME voltage coefficient α_E. The frequency dependence of α_E shows a resonance character at the electromechanical resonance for PZT in the bilayer. The resonance frequency depends on R, mechanical compliances, density, and the coefficient of electromechanical coupling for radial mode. The peak value of α_E and the width of resonance are determined by effective composite parameters. Theoretical estimates of α_E vs. f (not shown here) are in agreement with the data in Fig. 6.

Conclusion

The nature of magnetoelectric interactions have been investigated in bilayers consisting of sol–gel prepared ferromagnetic lanthanum strontium manganite and piezoelectric

PZT and in single crystal LSMO-PZT. In polycrystalline bilayers, maximum ME coupling is measured when (i) bilayers contained manganites processed by hot-pressing and sintered at 1580–1630 K and (ii) a slow-dry epoxy was used to bond LSMO and PZT. The bonding techniques are necessary to overcome problems, such as impurities at the interface, encountered in sintered bilayers that led to weakening of the ME coupling. We measured a factor of 2–10 improvement in ME coupling compared to sintered bilayers and multilayer of LSMO-PZT [7]. The strongest ME effects are measured for single crystal LSMO-PZT. Data on ME coefficients have been obtained as a function of bias magnetic field, temperature, and frequency. Theoretical estimates of α_E vs. H are in very good agreement with the data. The bilayer shows a resonant ME coupling at frequencies corresponding to radial acoustic modes in the bilayer. A significant increase in the strength of ME coupling has been measured at EMR.

Acknowledgements The work at Oakland University was supported by grants from the National Science Foundation, the Army Research Office, and the Office of Naval Research.

References

1. Nan C-W, Bichurin MI, Dong S, Viehland D, Srinivasan G (2008) J Appl Phys 103:031101
2. Bichurin MI, Viehland D, Srinivasan G (2007) J Electroceramics 19:243
3. Zhai J, Xing Z, Dong S, Li J, Viehland D (2008) J Am Ceram Soc 91:351
4. Fiebig M (2005) J Phys D Appl Phys 38:R123
5. Lupeiko TG, Lisnevskaya IV, Chkheidze MD, Zvyagintsev BI (1955) Inorg Mater 31:1245
6. Srinivasan G, Rasmussen ET, Gallegos J, Srinivasan R, Bokhan YuI, Laletin VM (2001) Phys Rev B 64:214408
7. Mori K, Wuttig M (2002) Appl Phys Lett 81:100
8. Wan JG, Liu J-M, Chand HLW, Choy CL, Wang GH, Nan CW (2003) J Appl Phys 93:9916
9. Zhai J, Xing Z, Dong S, Li J, Viehland D (2006) Appl Phys Lett 88:062510
10. Xing ZP, Zhai JY, Dong S, Li JF, Viehland D (2008) Meas Sci Technol 19:015206
11. Ramirez AP (1997) J Phys Condens Matter 9:8171
12. Srinivasan G, Rasmussen ET, Levin BJ, Hayes R (2002) Phys Rev B 65:134402
13. Shimlzu Y, Murata T (1997) J Am Ceram Soc 80:2072
14. Rata AD, Herklotz A, Nenkov K, Schultz L, Doerr K (2008) Phys Rev Lett 100:076401
15. Vrejoiu I, Ziese M, Setzer A, Esquinazi PD, Birajdar BI, Lotnyk A, Alexe M, Hesse D (2008) Appl Phys Lett 92:152506
16. PZT used in the study: sample No. APC850. American Piezo Ceramics, Inc., Mackeyville, PA
17. Srinivasan G, Rasmussen ET, Hayes R (2003) Phys Rev B 67:014418
18. Khapikov A, Uspenskaya U, Bdikin I, Mukovskii Ya, Karabashev S, Shulyaev D, Arsenov A (2000) Appl Phys Lett 77:2376
19. Bichurin MI, Petrov VM, Kiliba YuV, Srinivasan G (2002) Phys Rev B 66:134404
20. Zeng M, Wan JG, Wang Y, Yu H, Liu J-M, Jiang XP, Nan CW (2004) J Appl Phys 95:8069
21. Dong S, Cheng J, Li JF, Viehland D (2003) Appl Phys Lett 83:4812
22. Bichurin MI, Fillipov DA, Petrov VM, Laletsin U, Paddubnaya N, Srinivasan G (2003) Phys Rev B 68:132408